

$(h_{11/2})^2$ alignments in neutron-rich ^{132}Ba with negative-parity pairs

Y. Lei (雷杨)^{1,*} and Z. Y. Xu (徐正宇)²

¹Key Laboratory of Neutron Physics, Institute of Nuclear Physics and Chemistry, China Academy of Engineering Physics, Mianyang 621900, China

²INPAC, Physics Department, Shanghai Jiao Tong University, Shanghai 200240, China

(Received 1 March 2015; revised manuscript received 10 June 2015; published 23 July 2015)

The shell-model collective-pair truncation with negative-parity pairs is adopted to study the $(h_{11/2})^2$ alignment in ^{132}Ba . The proton $(h_{11/2})^2$ -alignment state is predicted as an $E \sim 4.6$ MeV and $\tau \sim 0.5$ μs isomer with relatively strong $E3$ decay channels. The oblately deformed neutron $(h_{11/2})^2$ alignment in the yrast band and four negative-parity bands are confirmed, even though two of these negative-parity bands favor the prolate deformation, which directly manifests the γ instability of ^{132}Ba .

DOI: 10.1103/PhysRevC.92.014317

PACS number(s): 21.10.Re, 21.60.Cs, 23.35.+g, 27.60.+j

I. INTERACTION

^{132}Ba is a typical γ -unstable nucleus in the transitional region of $Z \geq 50$ and $N \leq 82$ with a large variety of coexisting nuclear shapes. Its negative-parity bands with $I^\pi = 5^-$ and 6^- bandheads (bandhead energies 2.12 and 2.358 MeV, respectively) maintain an oblate shape, while prolately deformed negative-parity bands with $I^\pi = 7^-$ and 8^- bandheads (bandhead energies 2.902 and 3.105 MeV, respectively) were also reported in the ^{132}Ba level scheme [1,2]. There four negative-parity bands herein are denoted by 5^- , 6^- , 7^- , and 8^- bands, in sequence. In the yrast band, the $\tau = 8.94(14)$ ns 10^+ isomer is assigned as the neutron $(h_{11/2})^2$ alignment with an oblate shape. On the other hand, the proton $(h_{11/2})^2$ alignment with the prolate deformation is also expected in ^{132}Ba (unfortunately unobserved yet), because the competition between proton and neutron $(h_{11/2})^2$ alignments are generally exhibited in this nuclear region [3–12].

There may exist strong electromagnetic transitions from the $(\pi h_{11/2})^2$ -alignment state to states in 7^- and 8^- bands, because initial and final states share a similar prolate shape. It is desirable to theoretically estimate these transition rates before an experimental search for the $(\pi h_{11/2})^2$ alignment in ^{132}Ba .

The $(\nu h_{11/2})^2$ alignment was also suggested in 5^- , 6^- , 7^- , and 8^- bands according to their band irregularity around 5–6 MeV [1,2]. However, the experimental evidence is not as solid as the $(\nu h_{11/2})^2$ alignment in the yrast 10^+ isomer [13,14]. It is essential to confirm the $(\nu h_{11/2})^2$ alignment in these negative-parity bands from a shell-model perspective.

The present work aims at studying the $(h_{11/2})^2$ alignment in both positive and negative-parity states of ^{132}Ba within the shell-model framework. The model-space truncation is required to reduce the gigantic dimension of the shell-model description for ^{132}Ba . It is noteworthy that the collective-pair truncation of the shell model has proved to be an efficient approach for the $(h_{11/2})^2$ -alignment description [15–17]. In such a truncation, collective pairs with spin $0\hbar$ and $2\hbar$ are normally employed to represent the low-lying collectivity

[18–24], which can readily provide $\Delta I = 2$ band structures in the 5^- , 6^- , 7^- , and 8^- bands of ^{132}Ba . Recently, negative-parity pairs were introduced into the pair truncation [25–27], which enables a shell-model description of negative-parity states in a heavy even-nucleon system, e.g., negative-parity states of ^{132}Ba discussed here. Thus, the collective-pair truncation with negative-parity pairs is adopted for our negative-parity-state related study on the $(h_{11/2})^2$ alignment of ^{132}Ba .

II. CALCULATION FRAMEWORK

Our calculation adopts a phenomenological shell-model Hamiltonian as in Ref. [16]:

$$H = - \sum_{\sigma=\pi,\nu} \left(\sum_j \varepsilon_{j\sigma} \hat{n}_{j\sigma} + \sum_{s=0,2} G_\sigma^s \mathcal{P}_\sigma^{s\dagger} \cdot \tilde{\mathcal{P}}_\sigma^s + \kappa_\sigma \mathcal{Q}_\sigma \cdot \mathcal{Q}_\sigma \right) + \kappa_{\pi\nu} \mathcal{Q}_\pi \cdot \mathcal{Q}_\nu, \quad (1)$$

with

$$\begin{aligned} \mathcal{P}^{0\dagger} &= \sum_a \frac{\sqrt{2a+1}}{2} (C_a^\dagger \times C_a^\dagger)^0, \\ \mathcal{P}^{2\dagger} &= \sum_{ab} q(ab) (C_a^\dagger \times C_b^\dagger)^2, \quad \mathcal{Q} = \sum_{ab} q(ab) (C_a^\dagger \times \tilde{C}_b)^2. \end{aligned} \quad (2)$$

In Eq. (2), $q(ab) = \langle a || r^2 Y^2 || b \rangle / r_0^2$, where r_0 is the oscillator parameter, $\sqrt{\hbar/(m\omega)}$. Hamiltonian parameters, i.e., $\varepsilon_{j\sigma}$, G_σ^s , κ_σ , and $\kappa_{\pi\nu}$ in Eq. (1), are also taken from Ref. [16] as listed in Table I.

Our pair-truncated shell-model space for ^{132}Ba is given by the coupling of three proton pairs and three (hole-like) neutron pairs in the 50–82 shell. These pairs can be formally defined by

$$A^{I^\pi\dagger} = \sum_{a \leq b} \beta_{ab}^{I^\pi} A^{I^\pi\dagger}(ab), \quad A^{I^\pi\dagger}(ab) = \frac{(C_a^\dagger \times C_b^\dagger)^{I^\pi}}{\sqrt{1 + \delta_{ab}}}, \quad (3)$$

*leiyang19850228@gmail.com

TABLE I. Hamiltonian parameters from Ref. [16] in MeV.

	$s_{1/2}$	$d_{3/2}$	$d_{5/2}$	$g_{7/2}$	$h_{11/2}$	
ε_π	2.990	2.708	0.962	0.000	2.793	
ε_ν	0.332	0.000	1.655	2.434	0.242	
G_π^0	G_π^2	G_ν^0	G_ν^2	κ_π	κ_ν	$\kappa_{\pi\nu}$
0.130	0.030	0.130	0.026	0.045	0.065	0.070

where C_a^\dagger is the creation operator of the a orbit. Thus, $A^{I^\pi\dagger}(ab)$ is a noncollective pair with two nucleons at a and b orbits; $A^{I^\pi\dagger}$ represents a collective pair with optimized structure coefficients, $\beta_{ab}^{I^\pi}$, to best describe the nuclear low-lying collectivity. Especially, $\beta_{ab}^{I^\pi=0^+}$ corresponds to the Cooper-pair structure due to the strong nuclear pairing collectivity, and is determined following the principle of projected-particle-number BCS theory [28]. Other $\beta_{ab}^{I^\pi}$ with $I^\pi \neq 0^+$ are obtained by the diagonalization in the $\nu = 2$ broken-pair model space [29]. More details about the determination of $\beta_{ab}^{I^\pi}$ are described in Ref. [30].

In our calculation, four types of pairs are adopted:

- (1) Following previous pair-truncation calculations [18–24], collective pairs with $I^\pi = 0^+$ and 2^+ are introduced.
- (2) Bandbeads of 5^- and 6^- bands correspond to the mixture of neutron $h_{11/2} \times s_{1/2}$ and $h_{11/2} \times d_{3/2}$ configurations [1,2]. In the 50–82 major shell, such a mixture can only emerge in collective $I^\pi = 5^-$ and 6^- neutron pairs. Thus, these two pairs are introduced to develop 5^- and 6^- bands, and denoted by 5^- and 6^- pairs.
- (3) 7^- and 8^- bands are built on the coupling of $h_{11/2}$ and $g_{7/2}$ protons [1,2]. Considering the short-range property of nuclear force, the coupling with total spin $I = 9$ should give the lowest binding energy [31]. Thus, the noncollective $(\pi h_{11/2} \times \pi g_{7/2})^{I^\pi=9^-}$ pair is introduced.
- (4) We take the $(\pi h_{11/2} \times \pi h_{11/2})^{I^\pi=10^+}$ pair to describe the $(\pi h_{11/2})^2$ alignment.

In previous pair-truncation calculations [15–17], the $(\nu h_{11/2})^{-2}$ alignment is represented by the $(\nu h_{11/2} \times \nu h_{11/2})^{I^\pi=10^+}$ pair. However, we do not introduce such a pair, because the coupling of two 5^- and/or 6^- pairs with total angular momentum $I \geq 10\hbar$ (denoted the $5^- \otimes 6^-$ coupling) can also describe the $(\nu h_{11/2})^{-2}$ alignment. To demonstrate this point, we list structure coefficients of 5^- and 6^- pairs in Table II, which suggests that the $5^- \otimes 6^-$ coupling are

TABLE II. Structure coefficients, i.e., $\beta_{ab}^{I^\pi}$ defined in Eq. (3), of 5^- and 6^- pairs.

	$I^\pi = 5^-$	$I^\pi = 6^-$
$ab = h_{11/2} \times s_{1/2}$	+0.551	+0.616
$ab = h_{11/2} \times d_{3/2}$	−0.832	+0.780
$ab = h_{11/2} \times d_{5/2}$	+0.038	+0.097
$ab = h_{11/2} \times g_{7/2}$	−0.050	+0.053

mainly constructed by two $s_{1/2}$ and/or $d_{3/2}$ neutrons along with two $h_{11/2}$ neutrons. These two $s_{1/2}$ and/or $d_{3/2}$ neutrons only provide little angular-momentum contribution, so that the $I \geq 10\hbar$ total angular momentum of the $5^- \otimes 6^-$ coupling almost comes from the remaining two $h_{11/2}$ neutrons. In other words, these two $h_{11/2}$ neutrons have to contribute $I \sim 10\hbar$ angular momentum, which forces them to rotate in alignment. Thus, the $(\nu h_{11/2})^{-2}$ alignment emerges within the $5^- \otimes 6^-$ coupling.

For ^{132}Ba with three valence proton pairs and three valence neutron-hole pairs in the 50–82 major shell, our proton or neutron pair-truncated basis is given by

$$|\tau_{\sigma=\pi,\nu}^J\rangle = ((A^{r_1\dagger} \times A^{r_2\dagger})^{(J_2)} \times A^{r_3\dagger})^{(J)}|0\rangle, \quad (4)$$

where $A^{r_1\dagger}$, $A^{r_2\dagger}$, and $A^{r_3\dagger}$ can be any type of pairs we described above. Proton and neutron bases are coupled together as $|\tau^{J=J_\pi \times J_\nu}\rangle = |\tau_\pi^{J_\pi}\rangle \times |\tau_\nu^{J_\nu}\rangle$. Hamiltonian matrix elements under $|\tau^J\rangle$ bases can be calculated with the formalism of Ref. [32]. These elements are denoted by H_{ij}^τ , where i and j are indexes to identify bases in the diagonalization algorithm. The Hamiltonian should be diagonalized under a set of linearly independent, normalized, and orthogonal bases, which can be constructed by the linear combination of $|\tau^J\rangle$ bases as described in Ref. [33]. In detail, we calculate the overlap matrix of $|\tau^J\rangle$ bases, and diagonalize it with a serial of eigenvalues (e_i) and corresponding eigenvector matrix elements (v_{ij}). The i th normalized and orthogonal basis is given by

$$|\phi_i^J\rangle = \frac{1}{\sqrt{e_i}} \sum_j v_{ij} |\tau_j^J\rangle. \quad (5)$$

To handle the overcompleteness, we neglect $|\phi_i^J\rangle$'s with $e_i = 0$, and reserved $|\phi_i^J\rangle$ bases construct the pair-truncated space for ^{132}Ba . Thus, the Hamiltonian matrix under $|\phi_i^J\rangle$ bases is produced by

$$H_{ij}^\phi = \frac{1}{\sqrt{e_i e_j}} \sum_{kl} v_{ik} v_{jl} H_{kl}^\tau, \quad (6)$$

and inputted into Hamiltonian diagonalization. Resultant wave functions are used for further calculations on electromagnetic properties and expectation values of the pair numbers.

The electromagnetic-transition operators adopted in our calculation are

$$\begin{aligned} T(E2) &= \sum_{\sigma=\pi,\nu} e_\sigma r_\sigma^2 Y_\sigma^2, T(E3) = \sum_{\sigma=\pi,\nu} e_\sigma r_\sigma^3 Y_\sigma^3, \\ T(M1) &= \sqrt{\frac{3}{4\pi}} \sum_{\sigma=\pi,\nu} g_{l\sigma} \vec{l}_\sigma + g_{s\sigma} \vec{s}_\sigma. \end{aligned} \quad (7)$$

Here, e_σ , $g_{l\sigma}$, and $g_{s\sigma}$ (in units of e and μ_N/\hbar) are the effective charge, orbital, and spin gyromagnetic ratios of valence nucleons, respectively. They are taken from Ref. [16] as $e_\pi = 2$, $e_\nu = -1$, $g_{\pi s} = 5.58 \times 0.7$, $g_{\nu s} = -3.82 \times 0.7$, $g_{\pi l} = 1.05$, and $g_{\nu l} = 0.05$.

III. RESULTS AND ANALYSIS

Figure 1 presents the calculated ^{132}Ba spectrum compared with the experimental one, including the yrast band, 5^- , 6^- ,

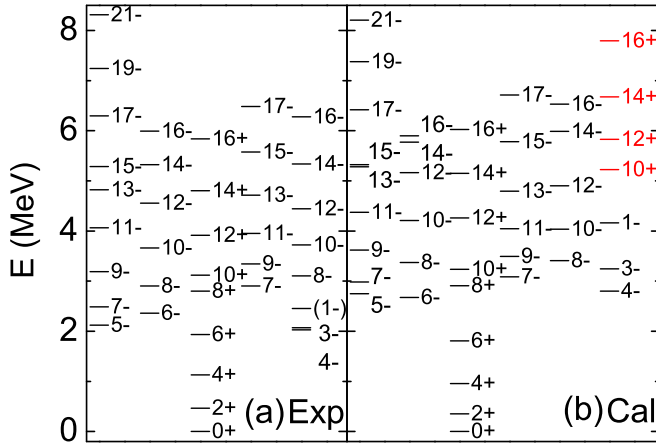


FIG. 1. (Color online) Experimental (a) [2,34] and the calculated spectrum (b), including the yrast band, 5^- , 6^- , 7^- , 8^- bands, and the $(\pi h_{11/2})^2$ -alignment band, which is highlighted in red.

7^- , 8^- bands and the potential $(\pi h_{11/2})^2$ -alignment band. A rough spectral consistency between our calculation and the experiment is achieved for these bands we are concerned about. One may also note that there is still inconsistency for low-lying 1^- , 3^- , and 4^- states, which are all out of our scientific motivation and our model space constructed with four types of pairs we itemize above [2,35,36]. Thus, we have no intention to fix the inconsistency by introducing redundant pairs, which obviously will complicate our study, and in what follows we limit ourselves to current model space. Furthermore, calculated 7^- and 8^- bands based on the $(\pi h_{11/2} \times \pi g_{9/2})^{I^\pi=9^-}$ pair are still observed to be systematically higher than those from experiments by ~ 0.3 MeV. This is because the single-particle energy of the ^{132}Ba $h_{11/2}$ proton, i.e., the $[550]_{1/2}^-$ level, is depressed by ~ 0.3 MeV relative to the Fermi surface [37], due to the $\beta_2 \sim 0.12$ prolate deformation of 7^- and 8^- bands [38]. This effect will also have direct impact on the prolate deformed $(\pi h_{11/2})^2$ alignment, which the shell-model framework cannot intrinsically consider yet. Therefore, our calculated excitation energy of the $(\pi h_{11/2})^2$ alignment should be reduced by ~ 0.6 MeV as an amendment. By searching the $(\pi h_{11/2} \times \pi h_{11/2})^{I^\pi=10^+}$ pair in output wave functions, the experimentally unobserved band beyond the $(\pi h_{11/2})^2$ alignment has been located in the calculated spectrum, as demonstrated by red levels in Fig. 1(b). The excitation energy of the corresponding 10^+ bandhead [i.e., the $(\pi h_{11/2})^2$ alignment] is $E \sim 5.2$ MeV. Thus, the ^{132}Ba $(\pi h_{11/2})^2$ -alignment energy is predicted to be around $4.6 = 5.2 - 0.6$ MeV, which agrees with the systematics of the alignment energy in light Ba isotopes [2,11,39].

To probe electromagnetic properties of the ~ 4.6 MeV $(\pi h_{11/2})^2$ -alignment state, we calculate its $E2$, $M1$, $E3$ decay to observed levels. Resultant $E2$ and $M1$ decay rates to yrast 8^+ , 10^+ , and 12^+ states are all smaller than 10^{-13} W.u. Such weak decays can be attributed to parity conservation, which forbids $E2$ and $M1$ transition operators from scattering the negative-parity $h_{11/2}$ nucleon to other positive-parity orbits of the 50–82 major shell. In other words, any state related to the $(\pi h_{11/2})^2$ alignment by strong $E2$ or $M1$ transitions must be

TABLE III. $E3$ transition rates (in W.u.) from the $I^\pi = 10^+$ isomer with the $(\pi h_{11/2})^2$ alignment to states in 7^- and 8^- bands. The superscript “*” labels the main decay branch.

J_f^π	$B(E3)$	J_f^π	$B(E3)$
7^-	0.008	8^-	0.145
9^-	0.109*	10^-	0.023
11^-	0.001	12^-	10^{-4}

constructed with two $h_{11/2}$ valence protons. However, yrast states, as well as most of low-lying positive-parity states in ^{132}Ba , have few valence $h_{11/2}$ protons due to the large $\pi h_{11/2}$ single-particle energy. Thus, strong $E2$ and $M1$ decays from the $(\pi h_{11/2})^2$ alignment to these low-lying positive levels are absent, which may partially explain the inaccessibility of the $(\pi h_{11/2})^2$ alignment in the observed level scheme of ^{132}Ba . On the other hand, we obtain relatively strong $E3$ decays from the $I^\pi = 10^+$ state with the $(\pi h_{11/2})^2$ alignment to states of 7^- and 8^- bands as shown in Table III. Such strong $E3$ decays are expected, because the $(\pi h_{11/2})^2$ alignment shares the prolate deformation with 7^- and 8^- bands. Based on above calculated decay rates, the $I^\pi = 10^+$ level with the $(\pi h_{11/2})^2$ alignment is suggested to be a $0.511 \mu\text{s}$ isomer with the main decay branch of $E_\gamma \sim 1.3$ MeV to the $I^\pi = 9^-$ level in the 7^- band.

Now, let us turn to the $(\nu h_{11/2})^2$ alignment. The yrast $I^\pi = 10^+$ isomer is the most typical $(h_{11/2})^2$ -alignment observation in ^{132}Ba . We would like to revisit the yrast alignment before discussing $(\nu h_{11/2})^2$ alignments in negative-parity bands. According to Fig. 1, our calculation spectrally reproduces the excitation energy of the yrast alignment. To present this alignment more explicitly, we additionally compare calculated and experimental associated energies $[E_I - E_{I-2}]$, reduced $E2$ transition rates $[B(E2, I \rightarrow I-2)]$, and magnetic g factors of the yrast band in Fig. 2. The backbending of $E_I - E_{I-2}$,

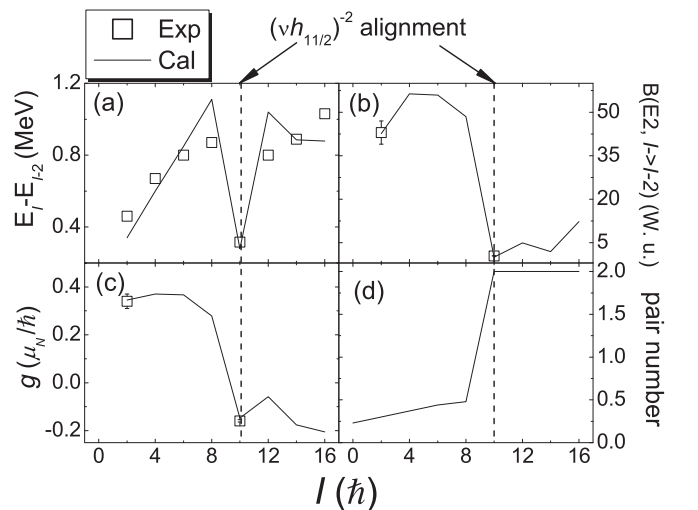


FIG. 2. $E_I - E_{I-2}$ (a), $B(E2, I \rightarrow I-2)$ (b), and g factors (c), as well as the sum of 5^- and 6^- pair numbers (d), of yrast states in ^{132}Ba from experiments (Exp) [34] and our calculation (Cal). The yrast $(\nu h_{11/2})^2$ alignment is highlighted.

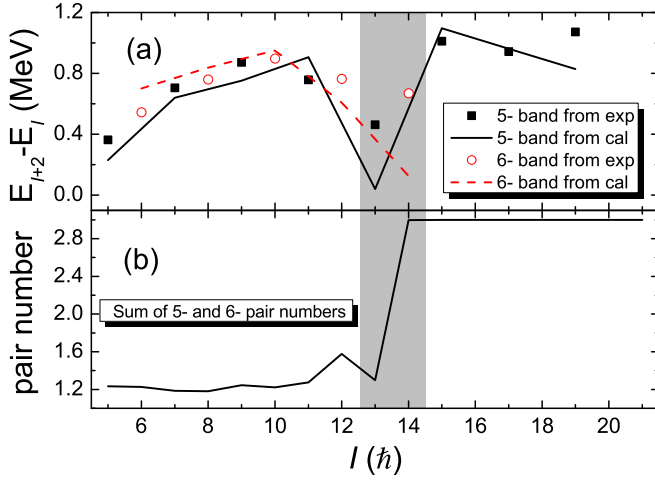


FIG. 3. (Color online) $E_{I+2} - E_I$ (a) and the sum of 5^- and 6^- pair numbers (b) in 5^- and 6^- bands. Abbreviations “exp” and “cal” correspond to the experimental data [34] and calculated results, respectively. The grey zone highlights the $(\nu h_{11/2})^{-2}$ alignment.

the sharp drop of $B(E2, I \rightarrow I - 2)$, and the g factor at the $I^\pi = 10^+$ isomer show both experimentally and theoretically the intrusion of the $(\nu h_{11/2})^{-2}$ alignment in the yrast band. To observe this alignment at the wave-function level, we also calculate the expectation value of 5^- and 6^- pair numbers, and plot the sum of 5^- and 6^- pair numbers in Fig. 2(d). Correspondingly to the $(\nu h_{11/2})^{-2}$ alignment at $I = 10\hbar$, two 5^- and/or 6^- pairs are suddenly excited as a representation of the $5^- \otimes 6^-$ coupling. In other words, the $(\nu h_{11/2})^{-2}$ alignment indeed is induced by the $5^- \otimes 6^-$ coupling. Therefore, we take the sudden increase of 5^- and 6^- pair numbers by 2 as a signal of the $(\nu h_{11/2})^{-2}$ alignment.

The $(\nu h_{11/2})^{-2}$ alignment in 5^- and 6^- bands was proposed according to the band irregularity around $I = 14\hbar$ in Refs. [1,2]. In Fig. 3(a), level spacings ($E_{I+2} - E_I$) also occur a sudden decrease around $I = 14\hbar$, and more implicitly demonstrate this band irregularity in both experimental and calculated level schemes. We present the sum of 5^- and 6^- pair numbers in Fig. 3(b) correspondingly. Below $I = 14\hbar$, only one 5^- or 6^- pair exists in 5^- and 6^- bands as expected by Ref. [1,2]; beyond this point, two more 5^- and/or 6^- pairs, i.e., the $5^- \otimes 6^-$ coupling, are excited. The $(\nu h_{11/2})^{-2}$ alignment in 5^- and 6^- bands is confirmed.

The $(\nu h_{11/2})^{-2}$ alignment is also expected in 7^- and 8^- bands around $I = 16\hbar$ [2], even though the spectral evidence

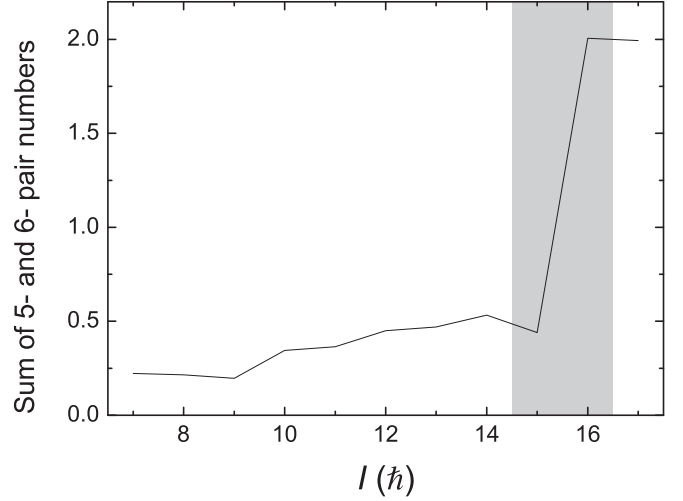


FIG. 4. Sum of 5^- and 6^- pair numbers in 7^- and 8^- bands. The grey zone highlights the potential $(\nu h_{11/2})^{-2}$ alignment.

was insufficient. We plot the sum of 5^- and 6^- pair numbers in 7^- and 8^- bands in Fig. 4, where the $5^- \otimes 6^-$ coupling is observed beyond $I = 16\hbar$. Thus, we confirm the $(\nu h_{11/2})^{-2}$ alignment with oblate shape in 7^- and 8^- bands, although these two bands favor the prolate deformation.

IV. SUMMARY

To summarize, we adopt the pair truncation of the shell model with negative-parity pairs to describe the $(h_{11/2})^2$ alignment in ^{132}Ba . Our calculation is spectrally consistent with experiments. The $I^\pi = 10^+$ state with the $(\pi h_{11/2})^2$ alignment is predicted to be an $E \sim 4.6$ MeV and $\tau \sim 0.5 \mu\text{s}$ isomer with relatively strong $E3$ transitions to 7^- and 8^- bands, which requires further experimental verification. $(\nu h_{11/2})^{-2}$ -alignment observations in both the yrast band and negative-parity bands are also well reproduced by the $5^- \otimes 6^-$ coupling, which is suggested to be another representation of the $(\nu h_{11/2})^2$ -alignment configuration. This oblately deformed alignment in prolate-favored 7^- and 8^- bands typically evidences the γ unstability of ^{132}Ba .

ACKNOWLEDGMENTS

This work was supported by the National Natural Science Foundation of China under Grant No. 11305151. Discussion with Prof. Y. M. Zhao is greatly appreciated.

- [1] E. S. Paul, D. B. Fossan, Y. Liang, R. Ma, and N. Xu, *Phys. Rev. C* **40**, 1255 (1989).
- [2] S. Juutinen *et al.*, *Phys. Rev. C* **52**, 2946 (1995).
- [3] Sun Xianfu *et al.*, *Nucl. Phys. A* **436**, 506 (1985).
- [4] K. Schiffer *et al.*, *Nucl. Phys. A* **458**, 337 (1986).
- [5] E. S. Paul, C. W. Beausang, D. B. Fossan, R. Ma, W. F. Piel, Jr., P. K. Weng, and N. Xu, *Phys. Rev. C* **36**, 153 (1987).

- [6] E. S. Paul *et al.*, *Phys. Rev. C* **36**, 2380 (1987).
- [7] J. P. Martin *et al.*, *Z. Phys. A* **326**, 337 (1987).
- [8] K. Schiffer *et al.*, *Z. Phys. A* **327**, 251 (1987).
- [9] W. Starzecki *et al.*, *Phys. Lett. B* **200**, 419 (1988).
- [10] J. P. Martin *et al.*, *Nucl. Phys. A* **489**, 169 (1988).
- [11] R. Wyss *et al.*, *Nucl. Phys. A* **505**, 337 (1989).
- [12] D. Ward *et al.*, *Nucl. Phys. A* **529**, 315 (1991).

- [13] S. Harissopulos, A. Gelberg, A. Dewald, M. Hass, L. Weissman, and C. Broude, *Phys. Rev. C* **52**, 1796 (1995).
- [14] P. Das, R. G. Pillay, V. V. Krishnamurthy, S. N. Mishra, and S. H. Devare, *Phys. Rev. C* **53**, 1009 (1996).
- [15] K. Higashiyama, N. Yoshinaga, and K. Tanabe, *Phys. Rev. C* **65**, 054317 (2002).
- [16] K. Higashiyama, N. Yoshinaga, and K. Tanabe, *Phys. Rev. C* **67**, 044305 (2003).
- [17] T. Takahashi, N. Yoshinaga, and K. Higashiyama, *Phys. Rev. C* **71**, 014305 (2005).
- [18] Y. A. Luo, J. Q. Chen, and J. P. Draayer, *Nucl. Phys. A* **669**, 101 (2000).
- [19] Y. M. Zhao, S. Yamaji, N. Yoshinaga, and A. Arima, *Phys. Rev. C* **62**, 014315 (2000).
- [20] N. Yoshinaga and K. Higashiyama, *Phys. Rev. C* **69**, 054309 (2004).
- [21] L. Y. Jia, H. Zhang, and Y. M. Zhao, *Phys. Rev. C* **75**, 034307 (2007).
- [22] K. Higashiyama and N. Yoshinaga, *Phys. Rev. C* **83**, 034321 (2011).
- [23] H. Jiang, C. Qi, Y. Lei, R. Liotta, R. Wyss, and Y. M. Zhao, *Phys. Rev. C* **88**, 044332 (2013).
- [24] H. Jiang, Y. Lei, C. Qi, R. Liotta, R. Wyss, and Y. M. Zhao, *Phys. Rev. C* **89**, 014320 (2014).
- [25] Y. Lei, G. J. Fu, and Y. M. Zhao, *Phys. Rev. C* **87**, 044331 (2013).
- [26] N. Yoshinaga, K. Higashiyama, R. Arai, and E. Teruya, *Phys. Rev. C* **87**, 044332 (2013).
- [27] N. Yoshinaga, K. Higashiyama, R. Arai, and E. Teruya, *Phys. Rev. C* **89**, 045501 (2014).
- [28] B. F. Bayman, *Nucl. Phys.* **15**, 33 (1960).
- [29] K. Allart, E. Boeker, G. Bonsignori, M. Savoia, and Y. K. Gambhir, *Phys. Rep.* **169**, 209 (1988).
- [30] Z. Y. Xu, Y. Lei, Y. M. Zhao, S. W. Xu, Y. X. Xie, and A. Arima, *Phys. Rev. C* **79**, 054315 (2009).
- [31] R. F. Casten, in *Nuclear Structure from a Simple Perspective*, (Oxford University Press, New York, 2000), p. 100.
- [32] Y. M. Zhao, N. Yoshinaga, S. Yamaji, J. Q. Chen, and A. Arima, *Phys. Rev. C* **62**, 014304 (2000).
- [33] J. Q. Chen, *Nucl. Phys. A* **626**, 686 (1997).
- [34] Evaluated Nuclear Structure Data File Retrieval, <http://www.nndc.bnl.gov/ensdfl/>.
- [35] S. M. Burnett *et al.*, *Nucl. Phys. A* **432**, 514 (1985).
- [36] M. Waroquier and K. Heyde, *Nucl. Phys. A* **164**, 113 (1971).
- [37] B. Singh, R. Zywina, and R. B. Firestone, *Nuclear Data Sheets* **97**, 241 (2002).
- [38] R. Wyss, J. Nyberg, A. Johnson, R. Bengtsson, and W. Nazarewicz, *Phys. Lett. B* **215**, 211 (1988).
- [39] R. Ma, Y. Liang, E. S. Paul, N. Xu, D. B. Fossan, L. Hildingsson, and R. A. Wyss, *Phys. Rev. C* **41**, 717 (1990).